Chinese Chemical Letters 34 (2023) 108135

Contents lists available at ScienceDirect

Chinese Chemical Letters

journal homepage: www.elsevier.com/locate/cclet

PDLLA length on anti-breast cancer efficacy of acid-responsive self-assembling mPEG-PDLLA–docetaxel conjugates

Tao Liu[a,1], Hui Zou[a,1], Jingqing Mu[a], Xi Zhang[a], Guohua Liu[a], Na Yu[a], Bo Yuan[b], Xiaoyong Yuan[b,c,d,*], Xingjie Liang[e], Shutao Guo[a,*]

[a] Key Laboratory of Functional Polymer Materials of Ministry of Education, State Key Laboratory of Medicinal Chemical Biology, Institute of Polymer Chemistry, College of Chemistry, Nankai University, Tianjin 300071, China
[b] School of Medicine, Nankai University, Tianjin 300071, China
[c] Clinical College of Ophthalmology, Tianjin Medical University, Tianjin 300020, China
[d] Tianjin Key Laboratory of Ophthalmology and Visual Science, Tianjin Eye Institute, Tianjin Eye Hospital, Tianjin 300020, China
[e] CAS Center for Excellence in Nanoscience, CAS Key Laboratory for Biomedical Effects of Nanomaterials and Nanosafety, Chinese Academy of Sciences and National Center for Nanoscience and Technology of China, Beijing 100190, China

ARTICLE INFO

Article history:
Received 29 September 2022
Revised 29 December 2022
Accepted 3 January 2023
Available online 5 January 2023

Keywords:
Nanomedicine
Prodrug
Docetaxel
mPEG-PDLLA
Acid-sensitive

ABSTRACT

Engineering small-molecule drugs into nanoparticulate formulations provides an unprecedented opportunity to improve the performance of traditional chemo drugs, but suffers from poor compatibility between drugs and nanocarriers. Stimuli-responsive mPEG-PDLLA–drug conjugate-based nanomedicines can facilitate the exploitation of beneficial properties of the carrier and enable the practical fabrication of highly efficacious self-assembled nanomedicines. However, the influence of hydrophobic length on the performance of this type of nanomedicine is little known. Here we synthesized two acid-sensitive ketal-linked mPEG-PDLLA–docetaxel prodrugs with different lengths of PDLLA, and engineered them into self-assembled sub-20 nm micellar nanomedicines for breast cancer chemotherapy. We found that the nanomedicine consisting of a mPEG-PDLLA–docetaxel prodrug with the shorter length of PDLLA stood out due to its potent cytotoxicity, deep penetration into multicellular spheroids, and improved *in vivo* anticancer performance. Additionally, our prodrug-based nanomedicines outperformed the generic formulation of commercial Nanoxel in terms of safety profile, tolerated doses, and tumor suppression. Our findings indicate that the hydrophobic content of a polymeric prodrug nanomedicine plays an important role in the performance of the nanomedicine, and should be instructive for developing polymeric prodrug-based nanomedicines with clinical translational potential.

Exploiting the advantages of nanotechnology, engineering small-molecule drugs into nanoparticulate formulations (*i.e.*, nanomedicines) provides an unprecedented opportunity to enhance the performance of traditional chemotherapeutic drugs and to screen new drug candidates [1–4]. Conventionally, encapsulation of hydrophobic drugs into the matrix of the hydrophobic part of an amphiphilic copolymer represents a simple and appealing strategy for nanomedicine fabrication [5]. For instance, methoxy polyethylene glycol-*block*-poly(D,L-lactide) (mPEG-PDLLA), a biodegradable and biocompatible copolymer, has been successfully exploited to develop two taxane micellar formulations (Genexol for paclitaxel and Nanoxel for docetaxel (DTX)) [6], boosting the massive studies for developing nanomedicines of various drugs by using mPEG-PDLLA or its analogs [7]. However, limited success has been achieved because this strategy requires excellent compatibility between small-molecule drugs and amphiphilic carriers. Moreover, nanomedicines suffer from low loading efficiency and poor colloidal stability both *in vitro* and *in vivo* [8,9].

Strategies such as changing the composition of amphiphilic polymers (*e.g.*, ratios of hydrophobic combinations, the length of the hydrophobic segment, and the structure of the unit) [10,11], optimizing processing methods [10], and cross-linking the core [12] have been attempted to improve the compatibility between drugs and the core of the nanocarrier. Although microfluidic devices can considerably expedite the high-throughput screening of nanomedicines [13], the development of nanomedicines using the above-mentioned strategies is essentially formulation-driven and

* Corresponding authors.
E-mail addresses: yuanxy_cn@hotmail.com (X. Yuan), stguo@nankai.edu.cn (S. Guo).
[1] These authors contributed equally to this work.

https://doi.org/10.1016/j.cclet.2023.108135
1001-8417/

inherently inflexible. As an alternative, developing prodrug-based nanomedicines is a modular approach, and conjugating chemo drugs onto the polymers through a chemical linkage can avoid the poor compatibility issue [14]. More importantly, this approach can exploit the beneficial properties of nanocarriers and thus facilitate the development of highly efficacious nanomedicines. For example, mPEG-PDLLA can self-assemble into small-sized nanoparticles of appropriate composition, with strong barrier-penetrating capability [15]. Thus, mPEG-PDLLA–drug conjugates may enable the practical fabrication of highly efficacious nanomedicines without complex synthesis, and are therefore appealing. Although the structure–*in vivo* fate relationship of mPEG-PDLLA (and analogous polymers) and their physically drug-loaded nanomedicines are extensively studied, and some mPEG-PDLLA–drug conjugates have been reported [7,8,16–18], the influence of hydrophobic content on the performance of nanomedicines has, unexpectedly, rarely been investigated and revealed.

Here two mPEG-PDLLA-ketal-DTX prodrugs (DKPPs) were synthesized by conjugating DTX to the end of the PDLLA block of mPEG-PDLLA through a ketal linkage, using a copper-catalyzed azide–alkyne cycloaddition reaction. $mPEG_{2k}$-$PDLLA_{1.8k}$ and $mPEG_{2k}$-$PDLLA_{3.5k}$ were used to construct $DKPP_{1.8k}$ and $DKPP_{3.5k}$, respectively, which were further engineered to micellar sub-20 nm nanomedicines named $DKPP_{1.8k}$-Mic and $DKPP_{3.5k}$-Mic (Fig. 1). The size, acid-sensitivity, and *in vitro* and *in vivo* anticancer performance of DKPP-Mics were systematically investigated. We found that the hydrophobic content of DKPP significantly affected the anticancer performance of DKPP-Mic: A shorter length of PDLLA and a higher critical micelle concentration (CMC) led to better outcomes.

$DKPP_{1.8k}$ and $DKPP_{3.5k}$ were synthesized using the combinational methodology of an acid-catalytic ketal construction strategy [19] and click chemistry (Schemes S1–S3 in Supporting information). The hydrophilic content of $DKPP_{1.8k}$ and $DKPP_{3.5k}$ was 41 wt% and 30 wt%, respectively, which should confer different CMC values. The structure of these DKPPs was confirmed by NMR, in which the characteristic peaks of PEG (δ 3.6, ^{1}H NMR), PDLLA (δ 5.2, 1.5, ^{1}H NMR), and the ketal linkage (δ 102, ^{13}C NMR) were observed (Figs. S1–S3 in Supporting information). Our synthetic approach was straightforward to conduct and would be applicable to other hydroxyl–group-bearing hydrophobic drugs. Amphiphilic DKPP could self-assemble into micellar formulations with a surface composed of PEG and a core composed of DTX-ketal-PDLLA (Fig. 2a). DKPP-Mics were prepared by the nanoprecipitation method. For comparison, DTX-Mic was also prepared by physically encapsulating DTX into the core of mPEG-PDLLA micelles according to the preparation procedure of Nanoxel, a commercial micellar DTX formulation that uses $mPEG_{2k}$-$PDLLA_{1.8k}$ as the carrier [20]. Compared with DTX-Mic (4.8 wt%), the drug content of $DKPP_{1.8k}$-Mic (15.2 wt%) and $DKPP_{3.5k}$-Mic (11.4 wt%) is increased by 2.4–3.2-fold (Table S1 in Supporting information). More importantly, DKPP-Mics displayed reasonable colloidal stability and could be stored at 4 °C for two weeks, facilitating their use for intravenous administration. The hydrophobic content is a critical factor in regulating the hydrodynamic diameter of micelles. Compared with blank $mPEG_{2k}$-$PDLLA_{1.8k}$ Mic (12.7 nm), $DKPP_{1.8k}$-Mic demonstrated a similar size (13.6 nm), while DTX-Mic (15.5 nm) and $DKPP_{3.5k}$-Mic (18.6 nm) were slightly bigger (Fig. 2b, Fig. S4 and Table S1 in Supporting information). Meanwhile, the particle size was

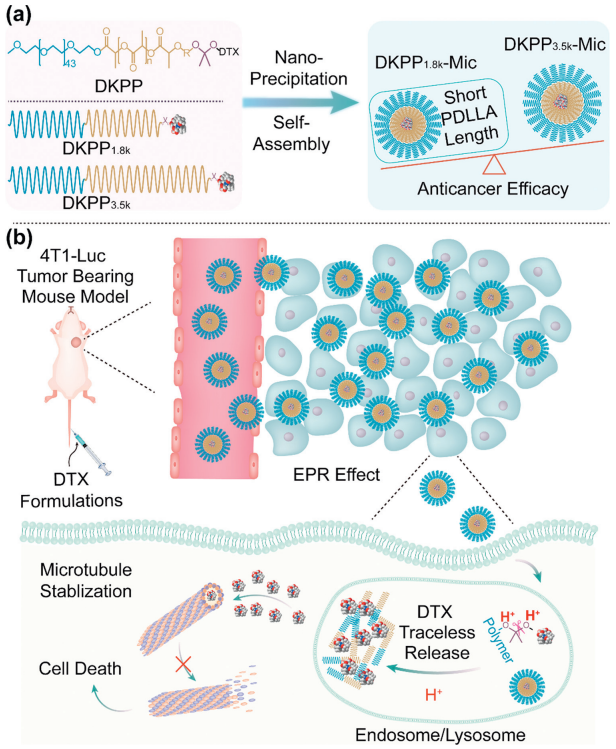

Fig. 1. Construction and evaluation of DKPP micellar nanomedicines (DKPP-Mics). (a) Two DKPPs were constructed with ketal linkage and self-assembled into micellar nanomedicines (DKPP-Mic) with different sizes due to the difference in PDLLA length. (b) Anticancer evaluation of DKPP-Mic in a subcutaneous 4T1-Luc breast cancer mouse model after intravenous injection, and the cancer cell-killing mechanism of DKPP-Mic.

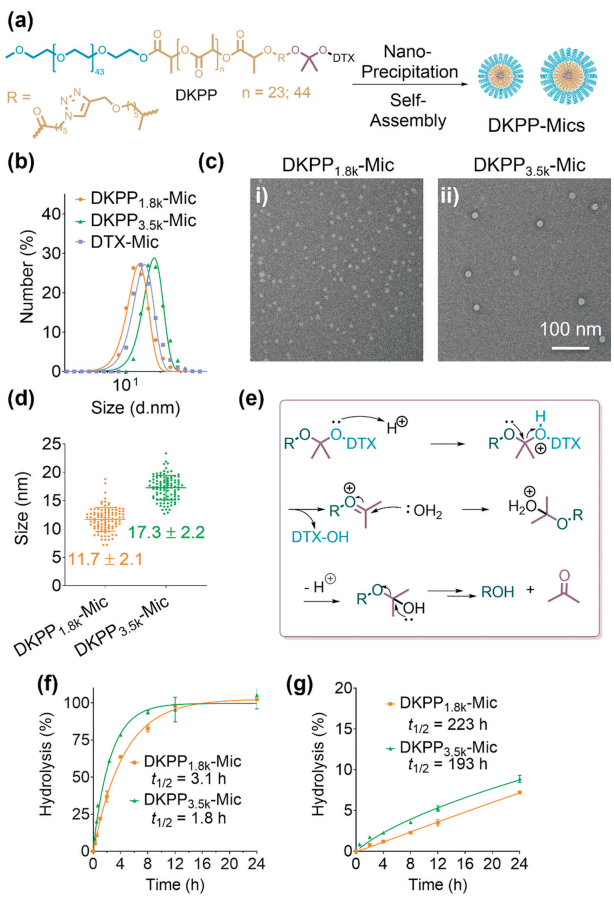

Fig. 2. Characterization of DTX formulations. (a) Preparation of DKPP-Mics using the nanoprecipitation technique. (b) DLS of DKPP-Mics and DTX-Mic. (c) TEM images of DKPP-Mics. (d) Size of micelles from (c); 100 micelles were measured. (e) Hydrolysis mechanism of DKPP. Hydrolysis curves of DKPP-Mics at (f) pH 5.0 and (g) pH 7.4. The half-life ($t_{1/2}$) of each DKPP is shown on the graph. Data are presented as means ± SDs ($n = 4$).

confirmed by TEM, and was slightly smaller than that determined by DLS (Figs. 2c and d, Fig. S5 in Supporting information). Besides, the PDIs of DKPP-Mics were about 0.3. Although DKPP did not carry any charge, DKPP-Mics exhibited negative zeta potentials because of the PEG surface (Table S1), which might facilitate their long blood circulation.

CMC can determine the colloidal stability of a micelle and is considered as an indicator of *in vivo* performance for physically drug-loaded micellar formulations [21]. Theoretically, micelles with lower CMC values will be more stable upon dilution and favorable for more prolonged blood circulation. Compared with unconjugated $mPEG_{2k}$-$PDLLA_{1.8k}$ (CMC = 3.19 μmol/L), the CMC of DTX conjugated $DKPP_{1.8k}$ (0.75 μmol/L) was markedly reduced by 4.2-fold because of a higher hydrophobic content (Table S1 and Fig. S6 in Supporting information). As expected, when the hydrophobic content was raised by increasing the PDLLA length, $DKPP_{3.5k}$ demonstrated a lower CMC value (0.51 μmol/L) than $DKPP_{1.8k}$.

Ketal-linked prodrugs may be activated in acidic environments to release native drug under the catalysis of acid (Fig. 2e). To study the hydrolysis kinetics of DKPP, DKPP-Mics at a concentration of 0.4 mmol/L (above the CMCs of DKPPs) were incubated in pH 5.0 buffer and pH 7.4 buffer, and the hydrolysis of DKPP was monitored by HPLC. After incubation for 8 h, more than 80% of DKPPs were hydrolyzed at pH 5.0 while less than 5% were hydrolyzed at pH 7.4, and the hydrolysis rate of DKPPs at pH 5.0 was 72–107 times faster than that at pH 7.4 (Figs. 2f and g, Fig. S7 and Table S2 in Supporting information). Compared with our previously reported PEGylated taxane prodrugs [22], DKPP-Mics demonstrated slower prodrug hydrolysis kinetics (3.5–5.7 times slower at pH 5.0), indicating that the introduction of the hydrophobic PDLLA segment endowed a more compact core and increased the colloidal stability. Surprisingly, we found that $DKPP_{3.5k}$-Mic with a higher hydrophobic content displayed faster hydrolysis kinetics than $DKPP_{1.8k}$-Mic. At pH 5.0 and pH 7.4, the $t_{1/2}$ values of $DKPP_{1.8k}$-Mic (3.1 h and 223 h, respectively) were 1.7-fold and 1.2-fold higher than those of $DKPP_{3.5k}$-Mic (1.8 h and 193 h, respectively), which may be attributed to a difference in the PEG chain density and conformation on the micellar surface. Compared with $DKPP_{1.8k}$-Mic, $DKPP_{3.5k}$-Mic was larger in particle size, with a lower density of PEG on the surface. PEG is probably in a "brush" configuration on the surface of $DKPP_{1.8k}$-Mic and extends away from the surface, whereas it is probably in a "mushroom" configuration on the surface of $DKPP_{3.5k}$-Mic and localizes more closely to the surface [23,24], facilitating the infiltration of protons into the core of the micelles to trigger ketal hydrolysis.

To evaluate the *in vitro* anticancer efficacy of DTX formulations, the cytotoxicity of DTX and DTX formulations against 4T1-Luc cells was assessed. DTX-Mic (IC_{50} = 14 nmol/L) displayed comparable cytotoxicity to DTX (IC_{50} = 13 nmol/L), while DKPP-Mics showed slightly decreased cytotoxicity (IC_{50} = 18 and 25 nmol/L) (Fig. 3a). The IC_{50} value of $DKPP_{3.5k}$-Mic (IC_{50} = 25 nmol/L) was 1.4 times higher than that of $DKPP_{1.8k}$-Mic (IC_{50} = 18 nmol/L) (Fig. 3a) even though $DKPP_{3.5k}$-Mic demonstrated faster *in vitro* hydrolysis kinetics; this may be attributed to a difference in cellular uptake profiles. DTX is an inhibitor of microtubule depolymerization [6]. To investigate the cell-killing mechanism of DKPP, 4T1-Luc cells were incubated with DTX or DTX formulations (500 nmol/L, 6 h), and the microtubules and nuclei were stained with tubulin-tracker-red and DAPI, respectively, for visualization using CLSM (Fig. 3b). Compared with untreated cells, in which microtubules were extended in the cytoplasm, cells treated with DTX and DTX formulations displayed higher proportions of cells with aggregated microtubules (Fig. 3b and Fig. S8 in Supporting information). To further investigate the cellular uptake of DKPP-Mics, 4T1-Luc cells were incubated with DKPP-Mic (10 μmol/L, 6 h). As shown in Fig. 3c, compared with $DKPP_{1.8k}$-Mic, $DKPP_{3.5k}$-Mic demonstrated a 1.4-fold lower cellular uptake of total equivalent DTX (C_{total}), which explains the low cytotoxicity of $DKPP_{3.5k}$-Mic. Besides, $DKPP_{1.8k}$-Mic and $DKPP_{3.5k}$-Mic displayed similar degrees of intracellular prodrug hydrolysis (91% and 87%, respectively), even though $DKPP_{3.5k}$-Mic demonstrated a faster *in vitro* hydrolysis rate in buffer solutions. These results indicate that DKPPs can be effectively activated inside the cell.

Nanoparticles with smaller sizes may achieve better penetration [25,26]. To investigate the *in vitro* tumor penetration of DKPP-Mics, 4T1-Luc multicellular 3D tumor spheroids were incubated with Cy5-labelled DKPP formulations (named ^{Cy5}DKPP-Mics, Scheme S4 in Supporting information) at 500 nmol/L for 12 h, and the penetration into spheroids and cellular uptake of ^{Cy5}DKPP-Mic were then determined by CLSM and flow cytometry, respectively. As visualized in Fig. 3d, $^{Cy5}DKPP_{1.8k}$-Mic penetrated more deeply into tumor spheroids. Meanwhile, we investigated the cellular uptake of ^{Cy5}DKPP-Mics by tumor spheroids. As shown in Figs. 3e and f, the proportion of Cy5-positive cells treated with $^{Cy5}DKPP_{1.8k}$-Mic (61.8%) was 2.3 times higher than that treated with $^{Cy5}DKPP_{3.5k}$-Mic (26.7%). These results indicated that compared with

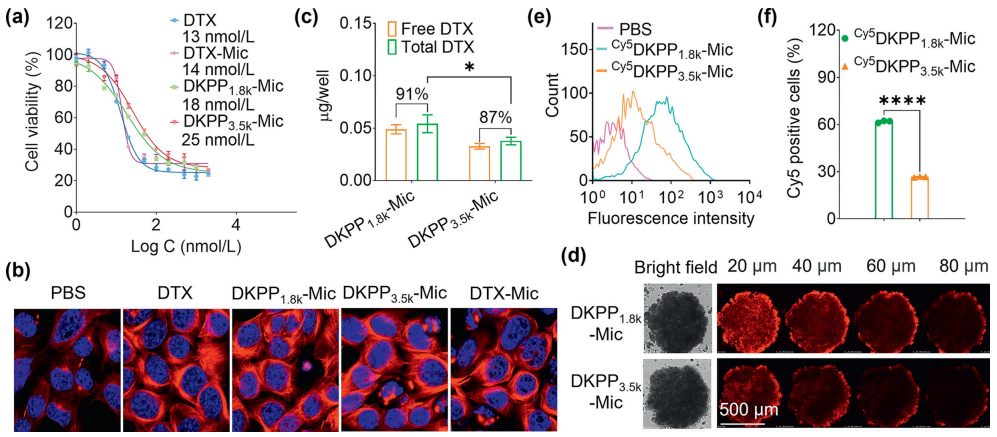

Fig. 3. *In vitro* evaluation of DTX formulations. (a) Cytotoxicity of DTX formulations against 4T1-Luc cells (n = 3). (b) 4T1-Luc cells were treated with drugs, and the microtubules and nucleus were stained with tubulin-tracker-red and DAPI, respectively (magnification: 800×). (c) Cellular uptake of drugs determined by HPLC (n = 4). Free DTX indicates the concentration of DTX released inside cells. The extent of hydrolysis (%) is indicated. (d, e) Multicellular 3D tumor spheroids were treated with ^{Cy5}DKPP-Mics (500 nmol/L, 12 h) to assess the penetration ability of DKPP-Mic by (d) CLSM and (e) flow cytometric analysis. (f) Percentages of Cy5-positive cells measured by flow cytometry (n = 3). Data are presented as means ± SDs; $^{*}P \le 0.05$; $^{****}P \le 0.0001$.

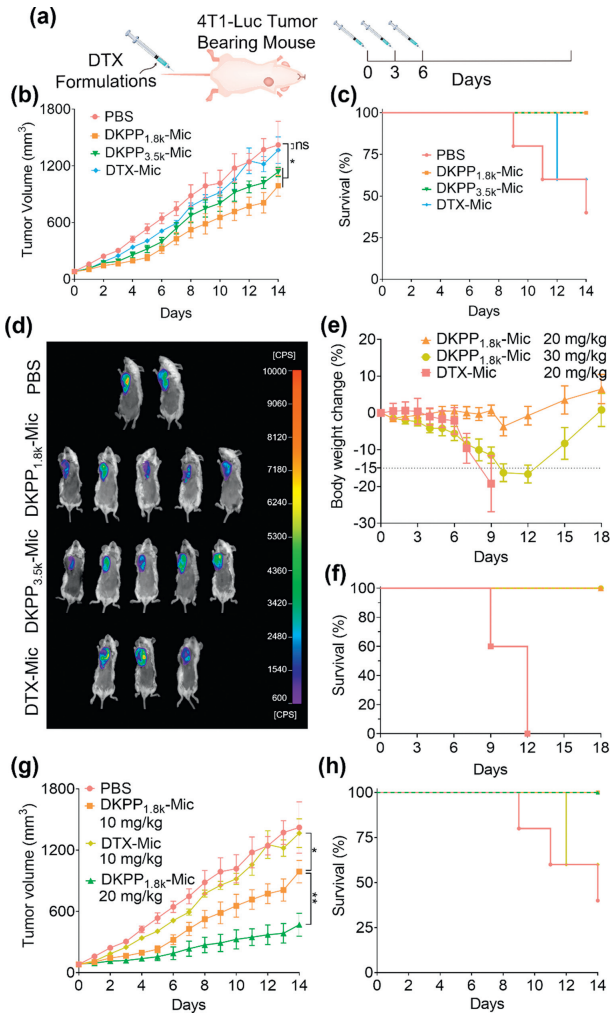

Fig. 4. *In vivo* anticancer evaluation of DTX formulations. (a) Establishment of 4T1-Luc breast tumor-bearing mouse model and the treatment schedule. (b) Tumor volume and (c) survival profiles were monitored every day. (d) IVIS luminescence imaging at the end of the experiment. The dose administered was 10 mg/kg (DTX equivalent dose). (e) Body weight and (f) survival profiles of mice during MTD evaluation. (g) Tumor volume and (h) survival profiles during anticancer treatment with DTX-Mic and $DKPP_{1.8k}$-Mic at their MTDs on 4T1-Luc tumor-bearing mice ($n = 5$). Data are presented as means ± SEMs; $^{*}P \leq 0.05$; $^{**}P \leq 0.01$; ns, not significant.

$DKPP_{3.5k}$-Mic, $DKPP_{1.8k}$-Mic demonstrated superior *in vitro* anticancer efficacy, with higher cellular uptake and deeper penetration in tumor spheroids.

We further evaluated the *in vivo* anticancer efficacy of DTX formulations using a 4T1-Luc tumor-bearing mouse model, and all animal protocols and experiments were carried out in accordance with the guidelines approved by the Institutional Animal Care and Use Committee of Nankai University. When tumors reached about 50 mm^3, mice were randomly divided into four groups and treated with PBS, $DKPP_{1.8k}$-Mic, $DKPP_{3.5k}$-Mic, or DTX-Mic at 10 mg/kg (DTX equivalent dose) every three days, for three doses, by tail vein injection (Fig. 4a). After 14 days, mice treated with DKPP-Mics demonstrated much delayed tumor growth and improved survival profiles compared with DTX-Mic-treated mice (Figs. 4b–d). The tumor inhibition rate of DTX-Mic, $DKPP_{1.8k}$-Mic, and $DKPP_{3.5k}$-Mic was 3.9%, 30.4%, and 20.1%, respectively (Fig. S9a in Supporting information). At the end of the experiment, no mice treated with DKPP-Mics had died, while two of five mice treated with DTX-Mic had died (Figs. 4c and d). Moreover, DKPP-Mics did not cause body weight loss in the mice, while the body weight of mice treated with DTX-Mic decreased dramatically (by 14% at the end of treatment) (Fig. S9b in Supporting information). Besides, $DKPP_{1.8k}$-Mic demonstrated better anticancer efficacy than $DKPP_{3.5k}$-Mic, consistent with the *in vitro* cellular experiments in which $DKPP_{1.8k}$-Mic was more cytotoxic and achieved better tumor spheroid penetration, possibly due to its smaller size [26].

$DKPP_{1.8k}$-Mic was used for subsequent investigation. To determine the maximum tolerated dose (MTD) of $DKPP_{1.8k}$-Mic and DTX-Mic, healthy BALB/c mice were treated with $DKPP_{1.8k}$-Mic and DTX-Mic at different dosages (Figs. 4e and f). We found that $DKPP_{1.8k}$-Mic could be administered up to 20 mg/kg (DTX equivalent dose) without causing mouse death or >5% body weight loss, while DTX-Mic caused dramatic body weight reduction (>15%) and death (5 of 5 mice died) at 20 mg/kg (DTX equivalent) (Fig. 4f). We next investigated the anticancer efficacy of $DKPP_{1.8k}$-Mic and DTX-Mic administered at their MTD doses (Figs. 4g and h), and found that tumors treated with DTX-Mic were about 2.8 times larger than those treated with $DKPP_{1.8k}$-Mic. The tumor inhibition rate of the $DKPP_{1.8k}$-Mic-treated group was improved from 30.4% to 61.9% when the dose increased from 10 mg/kg to 20 mg/kg (DTX equivalent dose) (Fig. S9a), indicating the outstanding anticancer potential of $DKPP_{1.8k}$-Mic.

Although PEG-PDLLA has been widely used as the carrier for constructing self-assembling polymer–drug conjugate-based nanomedicines [7], most studies have focused on improving drug loading, optimizing linker chemistry, targeting modification, topological design, and co-delivery of drug combinations. Theoretically, a lower CMC value indicates a more stable micellar core and improved colloidal stability, resulting in prolonged blood circulation and better anticancer efficacy. Previously, Lu *et al.* used $mPEG_{2k}$-$PLA_{4.2k}$ and $mPEG_{2k}$-$PLA_{8.9k}$ to construct two ester-linked mPEG-PLA–SN38 conjugates, investigated the impact of PLA length on the efficacy of prodrug-based nanomedicines, and found that conjugates with longer PLA had better anticancer efficacy [18], probably due to a lower CMC value and improved colloidal stability [21]. Coincidentally, our PEGylated cabazitaxel prodrug with a lower CMC value demonstrated better anticancer efficacy than that with a higher CMC value [22]. Nevertheless, in this study, $DKPP_{1.8k}$-Mic with a shorter PDLLA and higher CMC value showed better anticancer efficacy (Table S3 in Supporting information), perhaps due to its smaller size for enhanced penetration. Because CMC, which can be modulated by the length of PDLLA, has perplexing effects on the properties of nanomedicines, including circulation, accumulation, penetration, and cell uptake, the CMC of mPEG-PDLLA-drug conjugates should be delicately optimized in the design of highly efficacious nanomedicines.

In summary, two acid-responsive ketal-linked self-assembling mPEG-PDLLA–DTX conjugates were constructed, to improve DTX/carrier compatibility for facilitating DTX delivery and to investigate the impact of the length of PDLLA on the performance of prodrug-based nanomedicines. DKPPs were readily self-assembled into sub-20 nm nanomedicines with good acid-responsiveness. We found that $DKPP_{1.8k}$-Mic with a shorter PDLLA demonstrated better *in vitro* cytotoxicity, penetration in tumor spheroids, and *in vivo* anticancer efficacy. Besides, DKPP-Mics outperformed the generic formulation of commercial Nanoxel in anticancer efficacy and safety profile. Our nanomedicine platform would have broad applications in the delivery of various hydroxyl group-containing drugs or their combinations, and our findings offer new insights into constructing and optimizing acid-responsive polymeric prodrug nanomedicines.

Declaration of competing interest

The authors declare that they have no known competing financial interests or personal relationships that could have appeared to influence the work reported in this paper.

Acknowledgments

This work was financially supported by National Natural Science Foundation of China (Nos. 32171386 and 32201157), the Natural Science Foundation of Tianjin of China (No. 21JCZDJC01250), and the China Postdoctoral Science Foundation (No. 2021M690793).

Supplementary materials

Supplementary material associated with this article can be found, in the online version, at doi:10.1016/j.cclet.2023.108135.

References

[1] J. Shi, P.W. Kantoff, R. Wooster, O.C. Farokhzad, Nat. Rev. Cancer 17 (2017) 20–37.
[2] R. van der Meel, E. Sulheim, Y. Shi, et al., Nat. Nanotechnol. 14 (2019) 1007–1017.
[3] W. Wang, Q. Liu, C. Zhan, et al., Nano Lett. 15 (2015) 6332–6338.
[4] Y. Yuan, R. Bo, D. Jing, et al., Nano Res. 13 (2020) 503–510.
[5] R.A. Petros, J.M. DeSimone, Nat. Rev. Drug Discov. 9 (2010) 615–627.
[6] B. Sun, R.M. Straubinger, J.F. Lovell, Nano Res. 11 (2018) 5193–5218.
[7] F. Danhier, E. Ansorena, J.M. Silva, et al., J. Control. Release 161 (2012) 505–522.
[8] D. Hwang, J.D. Ramsey, A.V. Kabanov, Adv. Drug Deliv. Rev. 156 (2020) 80–118.
[9] Y. Zhao, F. Fay, S. Hak, et al., Nat. Commun. 7 (2016) 11221.
[10] J. Hrkach, D. Von Hoff, M.M. Ali, et al., Sci. Transl. Med. 4 (2012) 128ra139.
[11] L. Tan, J. Peng, Q. Zhao, et al., Theranostics 7 (2017) 2652–2672.
[12] S.Y. Lee, S. Kim, J.Y. Tyler, K. Park, J.X. Cheng, Biomaterials 34 (2013) 552–561.
[13] P.M. Valencia, O.C. Farokhzad, R. Karnik, R. Langer, Nat. Nanotechnol. 7 (2012) 623–629.
[14] I. Ekladious, Y.L. Colson, M.W. Grinstaff, Nat. Rev. Drug Discov. 18 (2019) 273–294.
[15] Y. Shi, S. Kim, T.B. Huff, et al., Nat. Nanotechnol. 5 (2010) 80–87.
[16] H.S. Yoo, T.G. Park, J. Control. Release 96 (2004) 273–283.
[17] Q. Shuai, G. Zhao, X. Lian, et al., Int. J. Pharm. 574 (2020) 118879.
[18] L. Lu, Y. Zheng, S. Weng, et al., Colloids Surf. B 142 (2016) 417–423.
[19] N. Yu, Y. Xu, T. Liu, et al., Nat. Commun. 12 (2021) 5532.
[20] S.W. Lee, M.H. Yun, S.W. Jeong, et al., J. Control. Release 155 (2011) 262–271.
[21] K. Zhang, X. Tang, J. Zhang, et al., J. Control. Release 183 (2014) 77–86.
[22] T. Liu, H. Zou, J.Q. Mu, et al., Chin. Chem. Lett. 32 (2021) 1751–1754.
[23] D.E. Owens 3rd, N.A. Peppas, Int. J. Pharm. 307 (2006) 93–102.
[24] T. Riley, C.R. Heald, S. Stolnik, et al., Langmuir 19 (2003) 8428–8435.
[25] J. Wang, W. Mao, L.L. Lock, et al., ACS Nano 9 (2015) 7195–7206.
[26] H. Cabral, Y. Matsumoto, K. Mizuno, et al., Nat. Nanotechnol. 6 (2011) 815–823.